SF2A 2011
G. Alecian, K. Belkacem, R. Samadi and D. Valls-Gabaud (eds)

ULTRA FAST VARIABILITY MONITORING WITH CTA

J. Biteau[1] and B. Giebels[1]

Abstract.
After three decades of small scale research, very high energy (> 100 GeV) gamma-ray astronomy emerged in 1989 with the detection of the Crab nebula by the Whipple observatory, Arizona, USA. In the '90s, French researchers improved the temporal and spatial sampling of the atmospheric showers initiated by gamma rays, with experiments such as ASGAT, Themistocle, Celeste and CAT. Only a handful of TeV sources had been seen in 2000, the Crab nebula (the standard candle in this field) and five extragalactic sources, mostly detected during flaring periods. The advent of stereoscopy (simultaneous monitoring of a shower with several telescopes) established the domain with observatories such as HEGRA and now H.E.S.S., in which French laboratories are involved. This enabled the detection of > 100 sources and the ability to sample light curves down to the minute time scale during exceptional outbursts, such as the flares of the blazar PKS 2155-304 in July 2006. During the next decade, the first large gamma ray observatory, CTA, will probe the sky above 50 GeV with tens of telescopes. The sensitivity and low-energy threshold of this array will allow the probing of blazar ultra fast variability during exceptional outbursts. We show with simulations that CTA timing capabilities would enable us to resolve the behaviour of PKS 2155-304 down to the second timescale, thus raising puzzling questions on the engine responsible for the TeV emission.

Keywords: high energy astrophysical phenomena, variability, galaxies: active, BL Lacertae objects: individual: PKS 2155-304

1 Introduction

Characteristic variability time scales of Active Galactic Nuclei (AGN) provide constraints on the properties of the emitting region. Assuming that the whole region of size R coherently emits the TeV γ rays, the causality argument yields a low bound on the minimum variability time scale $t_{var} > R/c \times (1+z)/\delta$, where δ and z are the Doppler factor and redshift of the studied region. Assuming that R scales with the Schwarzschild radius $R_S = 2GM/c^2$ of the supermassive black hole, one can derive a lower limit on the Doppler factor. Such constraints have been established by Aharonian *et al.* (2007) for the exceptional outbursts of PKS 2155−304 monitored by H.E.S.S. in July 2006. To derive proper variability time scales, the lightcurve shown on Fig. 1 was fitted with a series of generalized asymmetric gaussian peaks $\mathrm{I}(t) = A\exp[-(|t-t_{\max}|/\sigma_{r,d})^{\kappa}]$, where $t_{\max}$ is the time of the burst's maximum intensity A; σ_r and σ_d are the rise ($t < t_{\max}$) and decay ($t > t_{\max}$) time constants, respectively; and κ is a measure of the burst's sharpness. σ_r and σ_d being highly correlated with κ, the appropriate rise and decay times from half to maximum amplitude are then computed as $\tau_{r,d} = [\ln 2]^{1/\kappa}\sigma_{r,d}$. The peak finding and fitting procedure reveals that during MJD 59344 the flux of PKS 2155−304 is well described by a series five bursts above a constant term (see the table in Fig. 1, extracted from Aharonian *et al.*, 2007).

The shortest rise time during these outbursts is $\tau_r = 67 \pm 44$ s (fifth peak), with a large uncertainty due to the minute temporal binning. Conservatism impose to chose the shortest significant rise time as $\tau_{r\ HESS} = 173 \pm 28$ s (first peak), corresponding to a lower limit on the Doppler factor $\delta > 60-120$, for a black hole mass ranging in $1-2\times10^9 M_\odot$. Variability can also be investigated in the Fourier space. A structure function analysis of this lightcurve as well as the contiguous nights (Superina, 2008 - Abramowski *et al.*, 2010) shows that the Power Spectral Density (PSD) of the underlying stochastic process is well described by a power law $P_\nu \propto \nu^{-2}$. The high frequency part of the spectrum is almost flat above a frequency ν_{max}, i.e. dominated by the measurement uncertainty power, which would be lowered if the flux was measured with more statistics. Thus an improvement of the instrumental sensitivity would enable the probing of higher frequencies and bring better constraints on the shortest time scale visible in such a light curve.

[1] Laboratoire Leprince-Ringuet, Ecole Polytechnique, CNRS/IN2P3, F-91128 Palaiseau, France

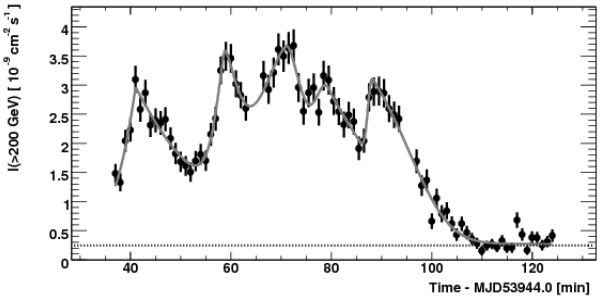

$t_{\max}$ [min]	A [10^{-9} cm^{-2} s^{-1}]	$\tau_{\rm r}$ [s]	$\tau_{\rm d}$ [s]	κ
41.0	2.7 ± 0.2	173 ± 28	610 ± 129	1.07 ± 0.20
58.8	2.1 ± 0.9	116 ± 53	178 ± 146	1.43 ± 0.83
71.3	3.1 ± 0.3	404 ± 219	269 ± 158	1.59 ± 0.42
79.5	2.0 ± 0.8	178 ± 55	657 ± 268	2.01 ± 0.87
88.3	1.5 ± 0.5	67 ± 44	620 ± 75	2.44 ± 0.41

Fig. 1. Left: Integral flux of PKS 2155−304 above 200 GeV during the first hours of MJD 59344. The data are binned in 1 min intervals. **Right:** Results of the best χ^2 fit of the superposition of five bursts and a constant to the H.E.S.S. data. The constant term is $0.27 \pm 0.03 \times 10^{-9}\,\mathrm{cm}^{-2}\,\mathrm{s}^{-1}$ (1.1 $\mathrm{I_{Crab}}$) *Extracted from Aharonian et al., 2007.*

2 Simulation of the lightcurves

2.1 Estimation of the flux

To estimate the flux that CTA would monitor, we first have to take into account the decrease of the energy threshold from $E_{min\ HESS} \sim 200$ GeV to $E_{min\ CTA} \sim 50$ GeV that would result in an increase of the integral flux above the threshold by a factor:

$$\Phi_{CTA}(t) = \Phi_{HESS}(t) \times \frac{\int_{E_{min\ CTA}}^{E_{max\ CTA}} F(E)\mathrm{d}E}{\int_{E_{min\ HESS}}^{E_{max\ HESS}} F(E)\mathrm{d}E} \tag{2.1}$$

where $E_{max\ HESS}$ and $E_{max\ CTA}$ are the maximum photon energies detectable by H.E.S.S. and CTA, reasonably approximated here as $+\infty$. $F(E)$, the photon spectrum - sometimes written dN/dE - is derived from the Synchrotron Self Compton (SSC) model fitted to the data of PKS 2155−304 during the 2008 multi wavelength campaign (Sanchez & Giebels, 2009 - Aharonian *et al.*, 2009). $\Phi_{HESS}(t)$ is the lightcurve shown on Fig. 1, reasonably approximated by the series of bursts described in the introduction.

The energy dependency of the flux is fully accounted for in Eq. (2.1), but the modeling of the time dependency requires knowledge on the small timescales behaviour of the flux and is thus related to the high frequency part of the PSD. If the temporal binning of the lightcurve monitored with CTA (resp. H.E.S.S.) is T_{CTA} (resp. T_{HESS}), then the highest frequency accessible for a given sampling (Nyquist frequency) will go from $\nu_{Nyq\ HESS} = 1/2T_{HESS}$ to $\nu_{Nyq\ CTA} = 1/2T_{CTA}$. The variability contained in the frequency range $[\nu_{Nyq\ HESS}, \nu_{Nyq\ CTA}]$, the extended part of the PSD, must be added to the lightcurve. Let us call the inverse Fourier transform of this extension $\Psi(t)$, then Eq. (2.1) becomes:

$$\Phi_{CTA}(t) = (\Phi_{HESS}(t) + \Psi(t)) \times \frac{\int_{E_{min\ CTA}}^{+\infty} F(E)\mathrm{d}E}{\int_{E_{min\ HESS}}^{+\infty} F(E)\mathrm{d}E} \tag{2.2}$$

To simulate $\Psi(t)$, a certain temporal behaviour must be assumed. One one hand, we assume no additional variability above the maximum frequency for which the H.E.S.S. PSD is significantly above the measurement noise level. Then, $\Psi(t)$ represents the measurement noise fluctuations. One the other hand, the PSD can be modeled as a continuous power law, even for frequencies above $\nu_{max\ HESS}$. Then $\Psi(t)$ Fourier transform is the extension of the H.E.S.S. PSD :

$$P(\nu) = \begin{cases} 0 & \text{if } \nu < \nu_{max\ HESS} \\ \\ \nu^{-2} & \text{if } \nu \geq \nu_{max\ HESS} \end{cases} \tag{2.3}$$

where $\nu_{max\ HESS} \sim 1.6 \times 10^{-3}$ Hz is the frequency for which the PSD of the HESS lightcurve is dominated by the measurement noise level. We use Timmer and König's method (1995) to simulate lightcurves associated to $P(\nu)$. One of the realizations is shifted to have a null mean and finally stretched to have a proper variance. The amplitude of the stretch is determined by the Parseval's theorem: the variance of the lightcurve points equals the area below the PSD. That is to say, if the PSD is described by a power law of Fourier index α:

$$V(\Phi_{CTA}) = V(\Phi_{HESS}) \times \frac{\int_{\nu_0}^{\nu_{max\ CTA}} \nu^{-\alpha}\mathrm{d}\nu}{\int_{\nu_0}^{\nu_{max\ HESS}} \nu^{-\alpha}\mathrm{d}\nu} \tag{2.4}$$

where ν_0 is the inverse of the lightcurve duration and $\nu_{max\ CTA}$ the frequency for which the PSD of the simulated CTA lightcurve is dominated by the measurement level noise, reasonably approximated by the associated Nyquist frequency *.

2.2 Estimation of the error on the flux and determination of the sampling rate

The estimation of the uncertainty on the flux in each time bin is of uttermost importance since it is directly related to the sampling rate. Assuming that the number of collected photons N_γ during a time T is Poisson distributed, the error on the integrated flux is $\sigma_{\Phi(>E_{min})} = \Phi(>E_{min})/\sqrt{N_\gamma}$.

To compute the integral flux above a threshold energy $\Phi(>E_{min})$, one has to take into account the energy dependency of the collection area, $A(E)$ obtained from simulations described by Bernlöhr (2008) / CTA consortium (2010), and weigh it by the energy distribution of the incoming photons $F(E)$:

$$\Phi(>E_{min}) = \frac{N_\gamma}{\left[\int_{E_{min}}^{+\infty} A(E)F(E)\mathrm{d}E \;/\; \int_{E_{min}}^{+\infty} F(E)\mathrm{d}E\right] \times T}. \tag{2.5}$$

The uncertainty on the integral flux is then :

$$\sigma_{\Phi(>E_{min})} = \sqrt{\frac{\Phi(>E_{min})}{\left[\int_{E_{min}}^{+\infty} A(E)F(E)\mathrm{d}E \;/\; \int_{E_{min}}^{+\infty} F(E)\mathrm{d}E\right] \times T}} \tag{2.6}$$

The last missing parameter in Eq. (2.6) is the temporal binning T, which is chosen so that the mean significance of CTA lightcurve points equals the one of H.E.S.S. lightcurve points.

3 Results

The lightcurve simulated in case of no extension of the PSD is shown in Fig. 2. The increase of collection area and decrease of energy threshold allows a temporal binning of few seconds vs a minute for the H.E.S.S. lightcurve. The analysis performed on the H.E.S.S. lightcurve by Aharonian *et al.* (2007) was applied to the CTA simulated one. This light curve was fitted with a series of bursts, detected with a peak finder, added to a constant term. The value of the latter parameter is fixed to $2.7 \times 10^{-9}\,\mathrm{cm}^{-2}\,\mathrm{s}^{-1}$, in agreement with the fit performed on H.E.S.S. data†. Each peak of the lightcurve shown in Fig. 2 is directly comparable to one of the H.E.S.S. lightcurve, since there is not any distortion by an additional variance. H.E.S.S. and CTA average rise/decay time resolution $\sigma_t =< \sigma_\tau \;/\; \tau >$ during the outburst can be derived from each table, yielding σ_t(H.E.S.S.)= 38% and σ_t(CTA)= 17%. This resolution improvement implies a significant measurement of the fifth peak rising time $\tau_{r\ CTA} = 60 \pm 18$ s, approximately three times smaller than $\tau_{r\ HESS} = 173 \pm 28$ s. Considering $\tau_{r\ CTA}$ as an upper limit on the variability time scale would yield a Doppler factor $\delta >$ 200 - 400.

In the case where variability is added above $\nu_{max\ HESS}$, the function $\Psi(t)$ can be derived from simulations, with power above the measurement noise level up to $\nu_{max\ CTA} \sim 10^{-2}$ Hz. One of the realization is used to obtain the simulated lightcurve $\Phi_{CTA}(t)$ shown in Figure 3. The addition of variance in the Fourier space yield substructures in the temporal space, the second and fourth peaks in this case, which could not have been resolved by H.E.S.S.. The shortest significant rising time tabulated in Fig. 3, $\tau_{r\ CTA} = 25 \pm 4$ s, is approximately seven times smaller than $\tau_{r\ HESS}$, corresponding to a Doppler factor $\delta > 450 - 900$, quite unusual within the currently favored acceleration schemes (Blandford, 2005). The large Doppler factor derived would certainly question the causality argument and the interpretation of such a lightcurve in terms of bursts.

*The PSD is a steep power law, which makes the variance in $[\nu_{max\ CTA}, \nu_{Nyq\ CTA}]$ negligible compared to the one in $[\nu_{max\ H.E.S.S.}, \nu_{max\ CTA}]$.

†C_{CTA} and C_{HESS} being the constant terms of each light curves, we fixed $C_{CTA} = C_{HESS} \times \int_{E_{min\ CTA}}^{+\infty} F(E)\mathrm{d}E / \int_{E_{min\ HESS}}^{+\infty} F(E)\mathrm{d}E$.

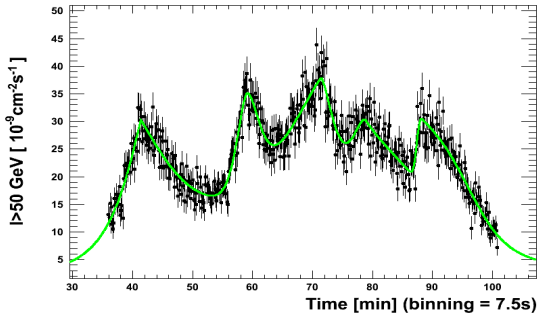

t_{max} [min]	A [10^{-9} cm^{-2} s^{-1}]	τ_r [s]	τ_d [s]	κ
41.4	26.7 ± 1.5	208 ± 13	452 ± 80	1.11 ± 0.17
59.1	16.8 ± 2.0	111 ± 14	138 ± 18	1.69 ± 0.63
71.5	32.7 ± 1.0	541 ± 106	186 ± 38	1.38 ± 0.27
78.8	23.8 ± 1.8	182 ± 36	784 ± 122	1.58 ± 0.81
88.3	11.9 ± 1.1	60 ± 18	513 ± 65	2.65 ± 0.40

Fig. 2. Left : Simulated integral flux of PKS 2155−304 above 50 GeV as CTA would monitor it. This simulation corresponds to the case where no additional variability is present above $\nu_{max\ HESS}$. The data are binned in 7.5 seconds intervals. **Right :** Results of the best χ^2 fit of the superposition of five bursts and a constant to the simulated CTA data. The constant term is fixed to $2.7 \times 10^{-9}\,\mathrm{cm}^{-2}\,\mathrm{s}^{-1}$.

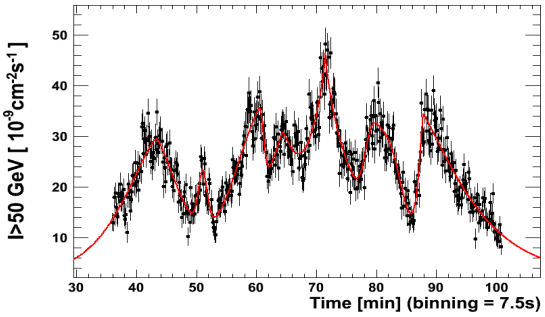

t_{max} [min]	A [10^{-9} cm^{-2} s^{-1}]	τ_r [s]	τ_d [s]	κ
43.3	25.7 ± 1.1	202 ± 13	147 ± 13	1.42 ± 0.15
51.0	10.9 ± 1.6	32 ± 8	34 ± 6	1.85 ± 0.44
60.4	17.5 ± 2.0	210 ± 19	37 ± 8	2.19 ± 0.35
64.4	15.1 ± 2.0	124 ± 27	60 ± 11	1.32 ± 0.28
71.5	43.7 ± 1.6	74 ± 9	80 ± 6	0.80 ± 0.11
80.5	18.3 ± 1.7	108 ± 17	177 ± 17	2.99 ± 0.43
87.8	26.8 ± 1.8	25 ± 4	235 ± 12	1.27 ± 0.10

Fig. 3. Left : Simulated integral flux of PKS 2155−304 above 50 GeV as CTA would monitor it. This simulation correspond to the case where variability is added above $\nu_{max\ HESS}$, assuming a PSD $P_\nu \propto \nu^{-2}$. The data are binned in 7.5 seconds intervals. **Right :** Results of the best χ^2 fit of the superposition of seven bursts and a constant to the simulated CTA data. The constant term is fixed to $2.7 \times 10^{-9}\,\mathrm{cm}^{-2}\,\mathrm{s}^{-1}$.

4 Conclusions

In July 2006, the H.E.S.S. collaboration observed an exceptional outburst of the blazar PKS 2155-304. The lightcurve sampling, limited by the instrumental sensitivity, revealed significant variations down to three minutes, imposing a Doppler factor above 60-120. The simulation of this dramatic outburst as it would be observed with the low energy threshold and the large collection area of CTA allows us to show that a gain of a factor ten on the sampling rate is achievable. Two scenarios of ultra-fast variability are investigated, each of them imposing a Doppler factor of several hundreds, quite unusual within the current blazar paradigm. The observation of such events with CTA will certainly raise puzzling questions on the mechanisms responsible for the TeV emission of blazars and will help to unravel their mysteries.

References

Abramowski *et al.* (H.E.S.S. Collaboration), 2010, A&A, 520, A83

Aharonian F. *et al.* (H.E.S.S. Collaboration), 2007, ApJ 664, L71

Aharonian F. *et al.* (H.E.S.S. & Fermi LAT collaborations) 2009, ApJL, 696, L150

Bernlöhr K., Astropart. Phys., 2008, 30, 149

Blandford R.D., 2005, Probing the Physics of AGN, ASP Conference Proceedings, San Francisco, Vol. 224, 499

CTA Consortium, 2010, arXiv:astro-ph/1008.3703

Sanchez D. and Giebels B., 2009, arXiv:0912.5152v1

Superina G., 2008, PhD thesis, Ecole Polytechnique

Timmer J., König M., 1995, A&A, 300, 707